

Liquid Crystalline Assembly of Rod–Coil Molecules

Ja-Hyoung Ryu · Myongsoo Lee (✉)

Center for Supramolecular Nano-Assembly and Department of Chemistry, Yonsei University, 120-749 Seoul, Korea
mslee@yonsei.ac.kr

1	Introduction	64
2	Diblock Rod–Coil Systems	65
2.1	Rod–Coil Diblock Copolymers Based on Perfectly Monodisperse Rods . . .	65
2.2	Rod–Coil Diblock Copolymers Based on Polydisperse Rods	71
2.3	Rod–Coil Diblock Copolymers Based on Peptide Rods	73
3	Triblock Rod–Coil System	75
3.1	ABC Coil–Rod–Coil Triblock Copolymers	75
3.2	ABA Coil–Rod–Coil Triblock Copolymers	79
3.3	BAB Rod–Coil–Rod Triblock Copolymers	86
3.4	Novel Rod–Coil Triblock Copolymers	87
4	Multiblock Rod–Coil System	90
4.1	Main-Chain Rod–Coil Copolymers	90
4.2	Side-Chain Rod–Coil Copolymers	92
5	Conclusions	94
	References	95

Abstract The development of novel supramolecular materials with nanometer-scale architectures and the effect of these architectures on the materials' properties are currently of great interest in molecular design. Liquid crystalline assemblies of rod-like mesogenic molecules containing flexible coils (rod–coil molecules) provide a facile entry into this area. Rod–coil molecules have been demonstrated to self-assemble into a rich variety of different liquid crystalline structures of nanoscale dimensions through the combination of shape complementarity and repulsive interaction of rigid and flexible parts as an organizing force. The mesophases include smectic, hexagonal or rectangular columnar, bicontinuous cubic, hexagonal channeled lamellar, barrel-like, honeycomb-like, and discrete micellar phases. The unconventional mesophases are induced by changing the rod-to-coil volume fraction, controlling the number of rod–coil repeating units, designing novel shapes of rod–coil molecules, and increasing the rod–coil molecular length.

Keywords Liquid crystal · Rod–coil · Self-assembly · Block copolymer · Microphase separation

1 Introduction

The development of new materials based on self-organizing systems has had a great deal of attention due to their potential in the construction of well-defined supramolecular nanostructures [1–6]. Self-assembling molecules, which include liquid-crystals [7–10], block copolymers [11–13], hydrogen bonded complexes [14, 15], and coordination polymers [16–18] are widely studied for their great potential as advanced functional materials. Especially, the construction of novel supramolecular architectures with well-defined shape and size by using rod building blocks is one of the most important subjects in organic materials chemistry because they can exhibit novel electronic and photonic properties as a result of both their discrete dimensions and three dimensional organization [19–22].

In contrast to organic molecules with low molecular weight, rod-coil systems consisting of rigid rod and flexible coil segments are excellent candidates for a large variety of ordered supramolecular structures covering several length-scales via a process of spontaneous organization [23, 24]. The rod-coil molecular architecture imparts microphase separation of the rod and coil blocks into ordered periodic structures in nanoscale dimensions due to the mutual repulsion of the dissimilar blocks and the packing constraints imposed by the connectivity of each block, while the anisometric molecular shape and stiff rod-like conformation of the rod segment imparts orientational organization. In order to balance these competing parameters, rod-coil molecules self-organize into a variety of supramolecular structures with domain sizes that general coil-coil copolymers could not show, and it can be controlled by variation of the rod-to-coil volume fraction [25–28]. Typical examples of the main types of rod-coil molecules forming supramolecular structures with mesophase are shown in Fig. 1. Basically, these rod-coil oligomers can be divided into two major classes: those containing monodisperse rod segments and those containing polydisperse rod parts.

In contrast to coil-coil block molecules, microphase separated structures in rod-coil block molecules can form, even though the molecular weight of each block is very small, due to large chemical differences between each block. The stiffness-asymmetry of rod-coil molecules that enhances the Flory-Huggins χ -parameter in comparison with coil-coil copolymers, results in well-ordered self-assembled structures of lower molecular weight. At the interface separation of the rod and coil domains, the relatively smaller area per junction favored by the rod block results in chain stretching of the coil block, which is energetically unfavorable. Considering the energetic penalties associated with chain stretching of the coil block and interfacial energy resulting from the interfaces separating the rod and coil domains, the theoretical works on rod-coil systems have predicted nematic-smectic A and smectic A-smectic C transitions in the melt [25, 26]. Other theoretical works

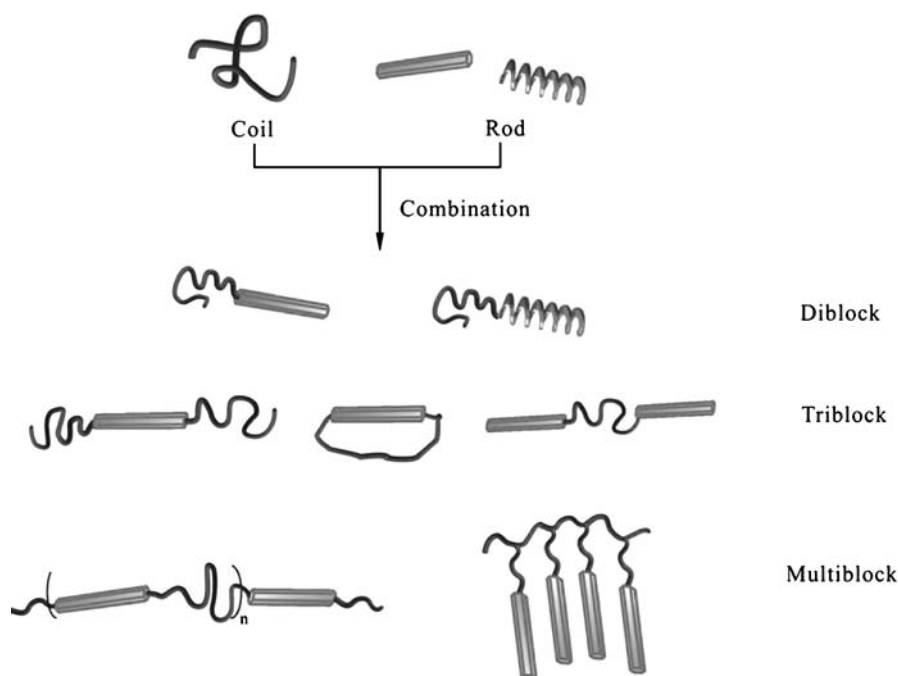


Fig. 1 Typical examples of rod-coil molecules

have dealt more with the phase behavior of rod-coil diblocks in a selective solvent for the coil segment [28]. These works have predicted various micellar structures for sufficiently large coil volume fractions, in addition to the familiar lamellar structures.

This chapter will present an overview of recent work in designing rod-coil systems, demonstrating their self-organization capability into a variety of liquid crystalline phases.

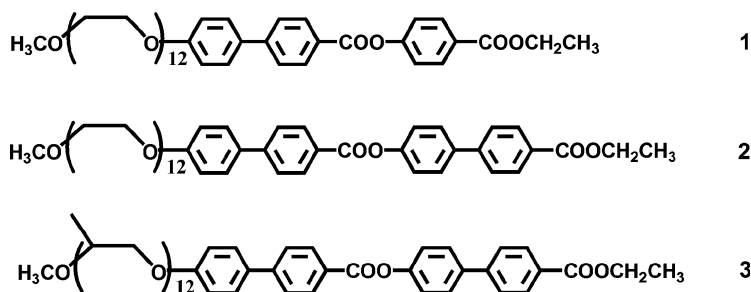
2

Diblock Rod-Coil Systems

2.1

Rod-Coil Diblock Copolymers Based on Perfectly Monodisperse Rods

It is well known that the connection of oligo(alkylene ether) chains into a calamitic rigid rod at the terminals destabilizes the thermotropic mesophases [8]. However, mesomorphic properties can be obtained by molecules with extended rigid rod segments as a result of the microphase segregation between the polar flexible oligo(alkylene oxide) ethers and rigid rod seg-



ments [2, 29]. The rod–coil molecules based on three phenyl units (1) as a rod segment, for example, exhibits only an isotropic phase after crystalline melting [30] while the molecule (2) based on four phenyl units as a rod segment shows a smectic A mesophase [29]. In the case of rod–coil molecule with short rod length, the coil segment may couple with the anisotropic rod owing to the relatively high miscibility between coil and rod segments, which can disturb the anisotropic aggregation of rod blocks. However, as the rod length increases, the immiscibility between chemically different flexible and rigid chains increases. This allows the increasing lateral intermolecular interactions of rigid segments. As a result, a layered smectic liquid crystalline phase can be induced, as exhibited by 2. If the coil volume fraction increases, smectic ordering of rod segments becomes unstable due to a large space crowding; consequently, the lamellar structure will transform into cylindrical micelles, which allows more volume for coils to explore. In contrast to the molecule 2, the molecule 3 based on a poly(propylene oxide) (PPO) coil shows a hexagonal columnar structure [31]. This large structural variation between the molecularly similar systems is probably caused by the larger spatial requirement of the bulkier PPO coil in comparison with the poly(ethylene oxide) (PEO).

In a systematic work on the influence of the coil length on phase behavior, rod–coil molecules (4) with PPO having different degrees of polymerization but the identical rod segment were prepared [32, 33]. A dramatic structural change in the mesophase of this rod–coil system was observed with variation in the coil length, as determined by a combination of techniques consisting of differential scanning calorimetry (DSC), optical polarized microscopy and X-ray scattering. Rod–coil molecules with seven propylene oxide (PO) repeating units exhibit a layered structure, while rod–coil molecules with 12 PO repeating units exhibit an optically isotropic cubic phase. This structure was identified by X-ray scattering methods to be a bicontinuous cubic (cub) structure with $Ia3d$ symmetry. Further increasing the coil length induces a hexagonal columnar mesophase, as in the case of the molecule with 20 PO repeating units (Fig. 2). Organization of the rod–coil molecules into a cross sectional slice of a cylinder for cubic and columnar phases gives rise to an aromatic core with approximately square cross section. The sizes and

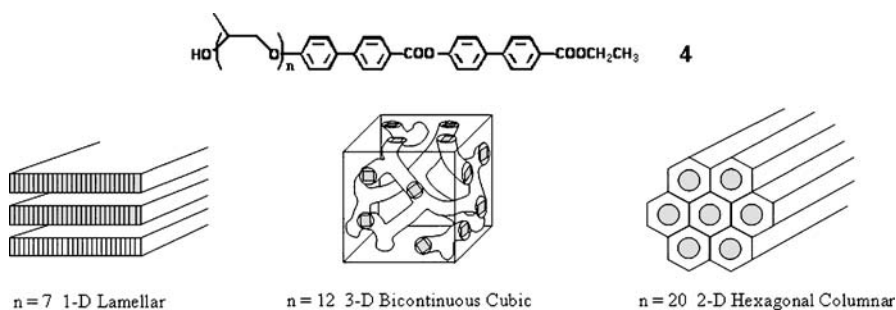


Fig. 2 Mesophases of the rod-coil diblock molecules by the increasing volume fraction of coil segments

periods of these supramolecular structures are typically in a range of less than 10 nm. This structural variation can be explained by considering the fact that increasing coil volume fraction leads to a structure with larger interfacial area, similar to the well-known conventional diblock copolymer phase behavior [13, 34, 35].

A strategy to manipulate supramolecular structures assembled from rod segments may be accessible by the alteration of the coil architecture (linear (5) versus branched (6)) in the rod-coil system [36]. On the basis of SAXS and TEM results, rod-coil molecules (5) with a linear PPO coil showed a honeycomb-like lamellar rod assembly with hexagonally arrayed PPO coil perforations, while the rod-coil molecules (6) with a dibranched PPO coil self-organized into rod-bundles with a body-centered tetragonal symmetry surrounded by a PPO coil matrix (Fig. 3). The notable feature is that a sim-

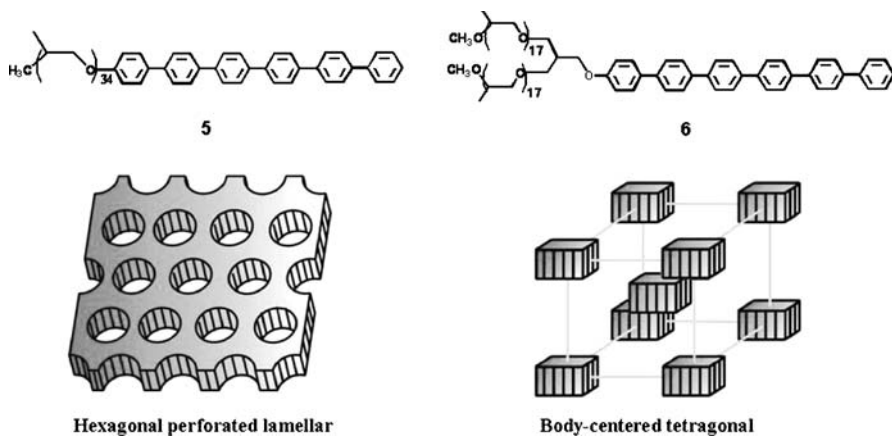


Fig. 3 3D supramolecular structural change from organized honeycombs (5) to organized bundles (6), dependent upon the coil architectural variation of the rod-coil molecule

ple structural variation from linear to dibranched chains generates a three-dimensional (3D) supramolecular structural inversion from organized coil perforations in rod layers to organized discrete rod bundles in a coil matrix. This implies that the steric hindrance at the rod/coil interface arising from branched coils plays a crucial role in the self-assembly of rod segments, as well as the conformational entropy associated with coil length.

Stupp et al. reported on rod-coil copolymers consisting of an elongated mesogenic rod and a monodisperse polyisoprene [37–39]. These rod-coil copolymers organize into ordered structures that differ in terms of varying rod volume fraction, as monitored by transmission electron microscopy and electron tomography. Depending on the rod volume fraction (f_{rod}), rod-coil oligomers either form strip-like morphologies or self-assemble into discrete aggregates that are organized in a hexagonal superlattice, with domain sizes typically between 5–10 nm. The authors also synthesized rod-coil copolymers containing oligostyrene-block-oligobutadiene as the coil block and rigid biphenyl units connected by ester linkages as the rod block [40–42]. Polarized optical microscopy showed that molecule 7 undergoes a phase transition from the smectic to the isotropic state. On the basis of TEM and X-ray data, it was suggested that the rod-coil molecules pack into the mushroom-shaped nanostructure with a height of 8 nm and a diameter of 2 nm. Each supramolecular nanostructure was estimated to contain approximately 23 molecules. Most importantly, this nanostructure was proposed to impart the spatial isolation of cross-linkable oligobutadiene blocks required to form a well-defined object. Therefore, polymerization might be confined to the volume of the supramolecular cluster. Thermal polymerization of rod-coil molecules in liquid crystalline state produced high molar-mass products with a very narrow polydispersity within a range of 1.15 to 1.25 and a molecular weight of approximately 70 000, as confirmed by GPC (Fig. 4). The macromolecular objects obtained reveal an anisotropic shape (2 by 8 nm) similar to that of supramolecular clusters, as determined by electron microscopy and small-angle X-ray scattering. Polarized optical microscopy showed that polymerization of the molecules into macromolecular objects results in a strong stabilization of the liquid crystalline phase that remains up to a chemical decomposition temperature of 430 °C. This result is interesting because the self-assembly process provides a direct pathway for preparation of well-defined molecular nanoobjects with distinct and permanent shapes through polymerization within supramolecular structures.

Yu et al. reported the synthesis of rod-coil block copolymers containing oligo(phenylene vinylene)s (OPV) coupled to either polyisoprene or poly(ethylene glycol) [43, 44]. These OPV showed a reversible thermotropic liquid-crystalline transition. The liquid-crystalline texture observed using a polarizing microscope shows a typical Schlieren pattern, which is evidence for the presence of nematic phases. TEM and small-angle X-ray scattering revealed alternating strips of rod-rich and coil-rich domains. The domain sizes

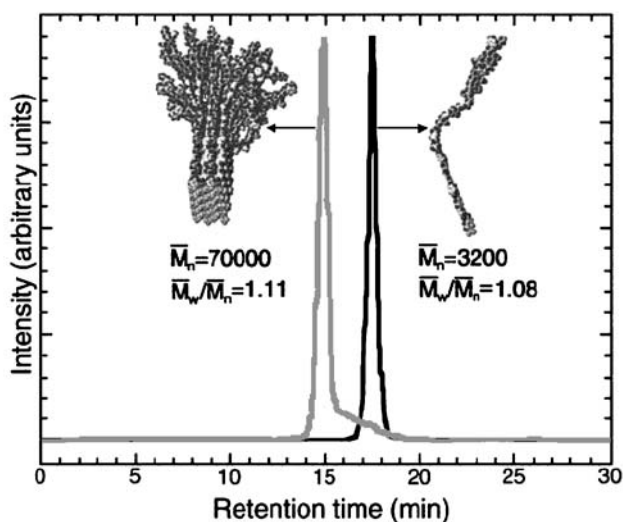
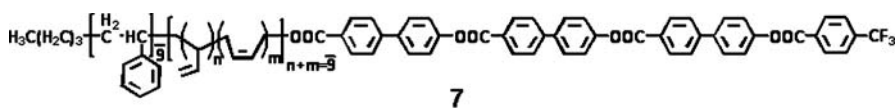


Fig. 4 GPC traces of rod-coil copolymer (7) and macromolecular object. Reprinted with permission from [40–42]. © 2001 American Association for the Advancement of Science

of the strips suggested that the supramolecular structures could be bilayer lamellar structures.

Incorporation of a rigid wedge-shaped building block into a diblock molecular architecture gives rise to a novel class of self-assembling systems consisting of a rigid wedge and a flexible coil because the molecule shares certain general characteristics of both dendrons and block copolymers. Lee et al. reported the self-assembling behavior of wedge-coil diblock molecules consisting of a rigid wedge and a flexible PEO coil in the melt state [45]. All of the molecules had a thermotropic liquid-crystalline structure after melting. The wide-angle X-ray diffraction patterns of all the molecules in the melt state are characterized by a diffuse scattering, which confirms their liquid-crystalline nature. However, a significant structural variation in the melt state was observed as the length of the PEO segment was varied, as evidenced by optical microscopic textures and small-angle X-ray diffraction patterns. The variation in the supramolecular structure can be rationalized by considering the microphase separation between the dissimilar parts of the molecule and the space-filling requirement of the flexible PEO chains (Fig. 5). The molecules based on a short PEO chain can be packed with a radial arrangement to fill the space efficiently, which results in a spherical supramolecular structure. Increasing the length of the PEO chain results in more space for

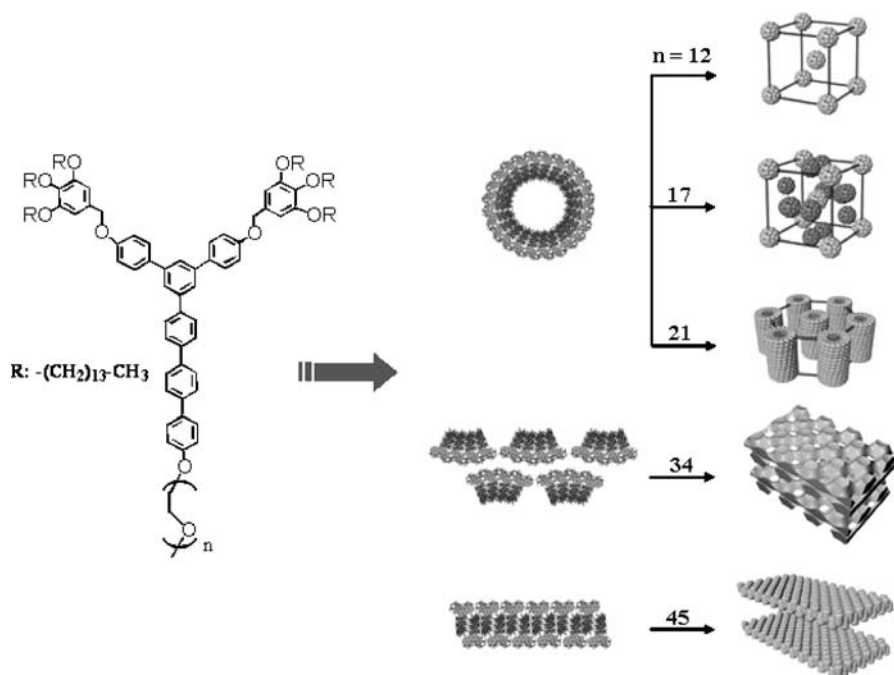


Fig. 5 Liquid crystalline structures formed by wedge-shaped molecules depend on the length of PEO

the chains being required while maintaining the radial arrangement of the rigid segments. Consequently, the discrete PEO domains will be extended to an infinitely long cylindrical domain in which the coils are less confined, which results in the formation of a 2D hexagonal columnar structure. Further increasing the length results in the rigid wedge-shaped segments assembling into a perforated lamellar structure with a radial arrangement of rigid segments, which allows a greater volume for the PEO chains to explore compared to that of the columnar structure. The radial arrangement of the wedge-shaped rigid segments eventually transforms into a parallel arrangement with interdigitation, to produce a flat interface while maintaining a constant density of the rigid hydrophobic domain. This transformation results in a monolayer lamellar structure as in the case of a molecule based on longest PEO chain.

Compared to other self-assembling systems based on dendritic molecules [46–48], the remarkable feature of the wedge-shaped building blocks investigated is their ability to self-assemble not only into spherical cubic and columnar structures, but also into an unusual bilayer lamellar structure with in-plane hexagonally ordered coil perforations. This approach of controlling supramolecular structures using wedge-shaped building blocks and only

a small variation in the length of grafted coils allows unexpectedly complex liquid crystalline structures to be produced.

2.2

Rod-Coil Diblock Copolymers Based on Polydisperse Rods

In contrast to the rod-coil diblock copolymer consisting of perfectly monodisperse rods, the liquid crystalline morphologies of rod-coil diblock copolymer containing polydisperse rods seem to be studied in less detail. In certain cases, the polydisperse nature of the rod-segments could hinder self-assembly into regularly ordered supramolecular structures. However, due to relatively simple synthetic procedures, liquid crystalline polymer can be of benefit for new materials with controlled internal dimensions ranging from the nanometer to macroscopic scale.

Poly(hexyl isocyanate) is known to have a stiff rod-like conformation in the solid state and in a wide range of solvents, which is responsible for the formation of a nematic liquid crystalline phase [49, 50]. The inherent chain stiffness of this polymer is primarily determined by chemical structure rather than by intramolecular hydrogen bonding. This results in a greater stability in the stiff rod-like characteristics in solution. The lyotropic liquid crystalline behavior in a number of different solvents was extensively studied by Aharoni et al. [51–53]. In contrast to homopolymers, interesting new supramolecular structures can be expected if a flexible block is connected to the rigid polyisocyanate block (rod-coil copolymers) because the molecule imparts both microphase separation characteristics of the blocks and a tendency of rod segments to form anisotropic order.

Thomas and coworkers reported rod-coil diblock copolymers consisting of poly(hexyl isocyanate) as the rod block and polystyrene as the coil block [54, 55]. A block copolymer consisting of poly(hexyl isocyanate) with DP of 900 and polystyrene with DP of 300 displays liquid crystalline behavior in concentrated solutions, suggestive of an anisotropic order of rod segments [54]. Transmission electron microscopy of bulk and thin film samples cast from toluene solutions showed the existence of a zigzag morphology with a high degree of smectic-like long range order. With additional research into the influence of the rod volume fraction on the phase behavior, the authors studied the rod-coil copolymers with varying compositions of rod blocks [55]. Transmission electron microscopy revealed phase-separated morphologies with rod-rich regions and coil-rich regions in which rod segments are organized into tilted layers analogous to those observed in smectic phases.

The authors also investigated the rod-coil block copolymer consisting of poly(3-(triethoxysilyl)propyl isocyanate) (23 kg/mol) (PIC) as a rigid rod and polystyrene (39 kg/mol) (PS) as a coil block [56]. Initial isotropic solutions of rod-coils undergo multiple ordering transitions until a final smectic microdomain structure develops in the dry state. The intermediate nematic

state is able to dynamically respond to external fields and form periodic defects. Depending on the evaporation of solvent, they showed that hierarchical morphology was induced in a rod-coil block copolymer film.

When the rod blocks contained reactive side groups with a composition having a large coil-to-rod volume ratio (PIC 23K, PS 200K), prism-like micelle nanoobjects could be synthesized via self-assembly of rod-coil diblock copolymers [57]. The PIC domain was cross-linked thermally via condensation of triethoxysilyl side groups and the rod directors remain parallel to each other due to the liquid crystalline order. Thermal cross-linking of the rod blocks only took place within each micellar nanodomain because the high molecular weight PS blocks could completely separate from each other. The TEM images indeed showed prism-like nanoobjects, which suggests a tilted bilayer structure consisting of 300 aggregates of the rod-coil block copolymer, as shown in Fig. 6. The result presents a novel method for forming anisotropic organic particles with potential multifacial surface characteristics.

De Boer et al. reported on the synthesis of a donor-acceptor, rod-coil diblock copolymer with the objective of enhancing the photovoltaic efficiency of the poly(phenylenevinylene)-C₆₀ system by incorporation of both components in a rod-coil molecular architecture that self-assembled through microphase separation [58]. These rod-coil copolymers showed nematic liquid crystalline phase and exhibit thermotropic transition at two regions. The first transition is attributed to the melting of the side chains, and the second higher one is an isotropic transition. Consequently, the diblock copolymers possess complex and rich phase behavior due to the combination of a mesogenic rod-like block and the adjacent coil-like block. The morphology of the polymer in bulk can play an important role in determining the photovoltaic cells, which the combination of a poly(*p*-phenylenevinylene)-type polymer as the donor material and C₆₀ as acceptor has effectively utilized.

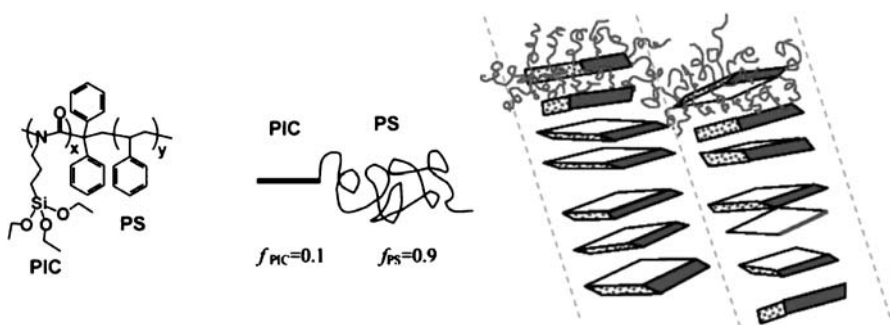


Fig. 6 Semectic ordering of the anisotropic nanoobjects formed from PIC(23K)/PS(200K). Reprinted with permission from [57]. © 2004 American Chemical Society

2.3

Rod-Coil Diblock Copolymers Based on Peptide Rods

Polymers with a stiff helical rod-like structure have many advantages over other synthetic polymers because they possess stable secondary structures due to cooperative intermolecular interactions. Examples of polymers with helical conformation are polypeptides in which the two major structures include α -helices and β -sheets. The α -helical secondary structure enforces a rod-like structure, in which the polypeptide main chain is coiled and forms the inner part of the rod [59]. This rod-like feature is responsible for the formation of the thermotropic and lyotropic liquid crystalline phases. Polypeptide molecules with α -helical conformation in solution are arranged with their long axes parallel to each other to give rise to a nematic liquid crystalline phase. However, even long chain polypeptides can exhibit a layered supramolecular structure when they have a well-defined chain length. For example, the monodisperse poly(α ,L-glutamic acid) prepared by bacterial synthetic methods assembles into smectic ordering on length scales of tens of nanometers [60, 61].

Incorporation of an elongated coil-like block to this helical rod system in a single molecular architecture may be an attractive way of creating new supramolecular structures due to its ability to segregate incompatible segments of individual molecules. The resulting rod-coil copolymers based on a polypeptide segment may also serve as models providing insight into the ordering of complicated biological systems. Low molecular weight block copolymers consisting of poly(γ -benzyl-L-glutamate) with DP of 10 or 20 and polystyrene with DP of 10 were synthesized by Klok, Lecommandoux, and a coworker [62]. Both the rod-coil polymers were observed to exhibit thermotropic liquid-crystalline phases with assembled structures that differ from the lamellar structures. Incorporation of a polypeptide segment into a polystyrene segment was observed to induce a significant stabilization of the α -helical secondary structure, as confirmed by FT-IR spectra. However, small-angle X-ray diffraction patterns indicated that α -helical polypeptides do not seem to assemble into hexagonal packing for the rod-coil copolymer with ten γ -benzyl-L-glutamate repeating units. The amorphous character of the polystyrene coil is thought to frustrate a regular packing of the α -helical fraction of the short polypeptide segments. Increasing the length of the polypeptide segment to a DP of 20 gives rise to a strong increase in the fraction of diblock copolymers with α -helical polypeptide segment. By studying this block copolymer with small-angle X-ray analysis, a 2D hexagonal columnar supramolecular structure was observed with a hexagonal packing of the polypeptide segments adopting an 18/5 α -helical conformation with a lattice constant of 16 Å. The authors proposed a packing model for the formation of the double-hexagonal organization. In this model, the rod-coil copolymers are assembled in a hexagonal fashion into infinitely long

columns, with the polypeptide segments oriented perpendicularly to the director of the columns. The subsequent supramolecular columns are packed in a superlattice with hexagonal periodicity parallel to the α -helical polypeptide segments, with a lattice constant of 43 Å.

In addition, the authors reported that two series of peptide rod-coil block copolymers based on γ -benzyl-L-glutamate or ε -benzyloxycarbonyl-L-lysine as a rod building block and a short oligo(styrene) (DP = 10) coil self-assembled into well-ordered structures, and that the conformation of the α -helical peptide rod is sensitive to temperature [63]. Under ambient conditions, the peptide segments of the diblock oligomers largely possess an α -helical secondary structure, indicating the rod-coil architecture of the molecules as confirmed by FT-IR spectra. For all molecules, increasing the length of the peptide segment results in a stabilization of the α -helical secondary structure and ultimately allows a regular organization of the rod-like peptide blocks. The small-angle X-ray diffraction pattern of peptide block copolymers based on short γ -benzyl-L-glutamate also indicates a columnar hexagonal arrangement, except for one composed of the shortest peptide segments ($n = 10$). However, in case of the long γ -benzyl-L-glutamate peptide segments ($n = 20, 40$), increasing temperature transforms the organized structure from hexagonal columnar into lamellar structure due to the change of the peptide conformation from

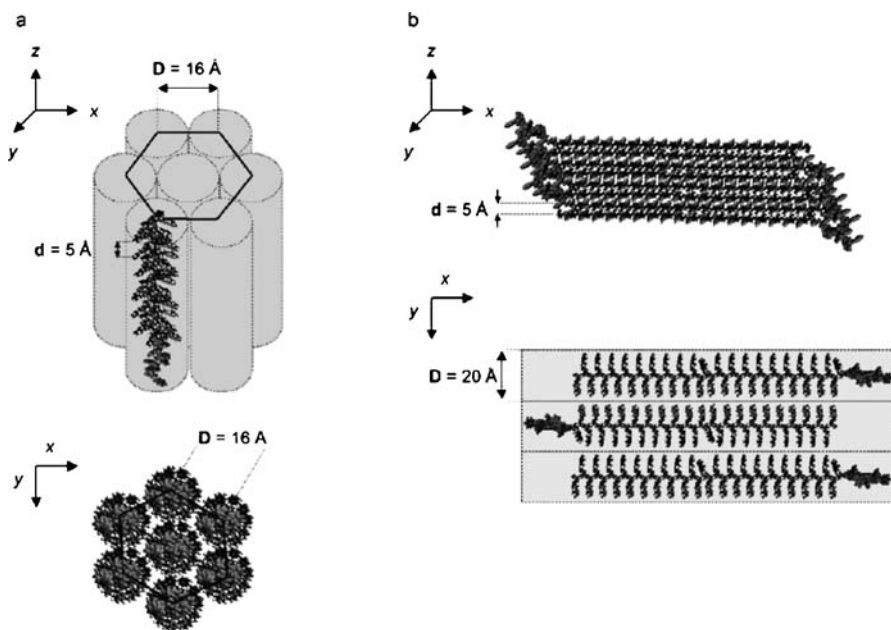


Fig. 7 **a** Columnar hexagonal and **b** lamellar β -sheet organization of the (styrene)₁₀-*b*-(γ -benzyl-L-glutamate)_{*n*} diblock oligomers (PS₁₀-*b*-PBLG_{*n*}). Reprinted with permission from [63]. © 2001 American Chemical Society

α -helix to β -sheet (Fig. 7). The block length required to allow such a transition varies from ~ 40 repeat units for the PS_{10} -*b*-PBLG_{*n*} diblock oligomers to ~ 80 α -amino acids for the PS_{10} -*b*-PZLys_{*n*} series, reflecting the lower α -helix-forming propensity of Z-Lys in comparison with Bn-Glu.

In contrast to peptide diblock copolymers based on general polymers, Deming and Pochan et al. reported on unique copolymers that are completely peptidic [64]. Leucine (L), racemic copolymers of L- and D-leucine (racL), or a random copolymer of L and valine (V) blocks with the inherent secondary structures of random coil (racL or LV) or rigid rod (L), were attached to PBLG molecules. In PBLG diblock copolymers with relatively small additional blocks, cholesteric liquid crystalline ordering was observed in bulk films. However, depending on the kinetics of film formation and the amount of non-PBLG block, the nanostructure or microstructure were able to be controlled. These purely peptidic block molecules can provide the opportunity to pattern materials with peptidic functionalities by taking advantage of block copolymer phase behavior and liquid crystal ordering.

Very recently, the self-assembly of poly(γ -benzyl-L-glutamate)-*b*-poly(L-lysine) rod-coil copolypeptide via ionic complexation was reported by Ikkala, Hadjichristidis and coworkers [65]. Complexation between the anionic surfactants dodecyl benzenesulfonic acid and the cationic poly(L-lysine) chains occurs via proton transfer from the acid group to the base, resulting in electrostatically bonded comb-like structures, and fluid-like liquid crystalline structures at room temperature due to efficient plasticization of dodecyl benzenesulfonic acid.

3

Triblock Rod-Coil System

3.1

ABC Coil-Rod-Coil Triblock Copolymers

If a chemically distinct hydrophobic chain is attached to the opposite ends of rod segment, segregation of incompatible chain ends takes place and leads to an ordered phase composed of three distinct sub-layers [66]. Coil-rod-coil ABC triblock molecules give rise to the formation of self-assembled structures with higher interfacial areas in comparison with AB diblock molecules. In contrast to that of diblock molecules based on a PEO coil, which show isotropic or smectic phase depending on the coil length, the ABC triblock molecule exhibits a hexagonal columnar mesophase [67]. Molecule (9) with 22 ethylene oxide (EO) repeating units, for example, exhibits hexagonal columnar mesophase which, in turn, undergoes transformation into a discrete spherical micellar structure in which rod segments are packed into a discrete bilayer lamellar structure that is encapsulated with PEO coils

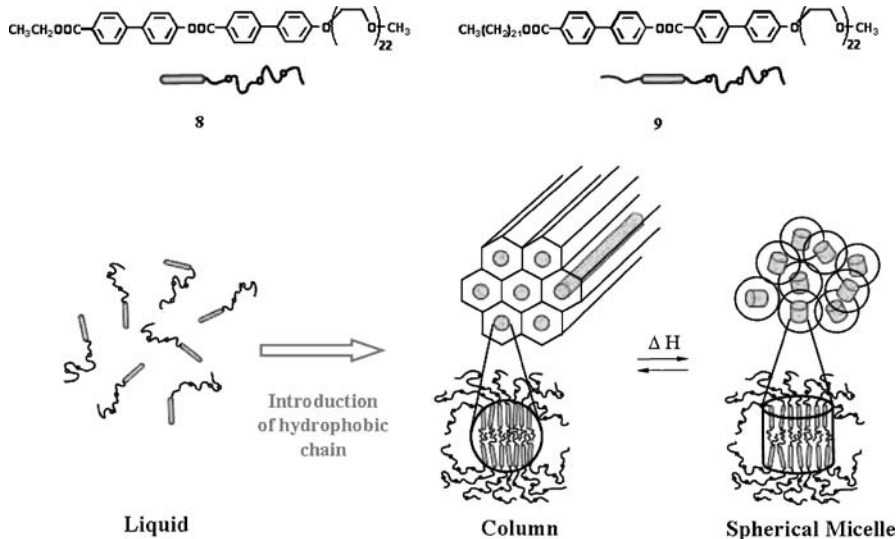


Fig. 8 Induction of the mesophase in rod-coil molecules via hydrophobic forces

(Fig. 8). Small-angle X-ray diffraction in the optically isotropic state revealed a strong primary peak together with a broad peak of weak intensity at about 1.8 relative to the primary peak position, indicating that the spatial distribution of centers of the spherical micelles has only liquid-like short range order, most probably due to random thermal motion of spherical micelles [68, 69]. From the observed primary peak of X-ray diffraction, the diameter of spheres was estimated to be approximately 12 nm. Considering that diblock rod-coil molecule (8) with 22 EO repeating units shows only an isotropic phase after crystalline melting, it is likely that hydrophobic forces play an important role in the self-assembly of the molecules into discrete nanostructures.

A novel strategy for manipulating the supramolecular nanostructure may be accessed by binding the C coil block of a coil-rod-coil ABC triblock molecule (9) into a tetrabranched triblock molecule (10) at a specific coil volume fraction [70]. This binding may slightly modify the entropic contribution of the coil C part in the coil-rod-coil ABC system. In comparison with the monomer, the tetramer has restricted chain end mobility through covalent linkage. Consequently, this effect may bring about the formation of a novel supramolecular nanostructure. Tetramerization of the molecule 9 provides an unusual example of the formation of a 3D tetragonally perforated lamellar liquid crystalline phase as an intermediate phase between conventional lamellar and columnar structures (Fig. 9). The supramolecular structure consists of liquid crystalline rod layers with in-plane tetragonally ordered coil perforations stacked in an AB-BA sequence. The perforations are likely to be filled by docosyl chains, most probably due to the large chemical difference

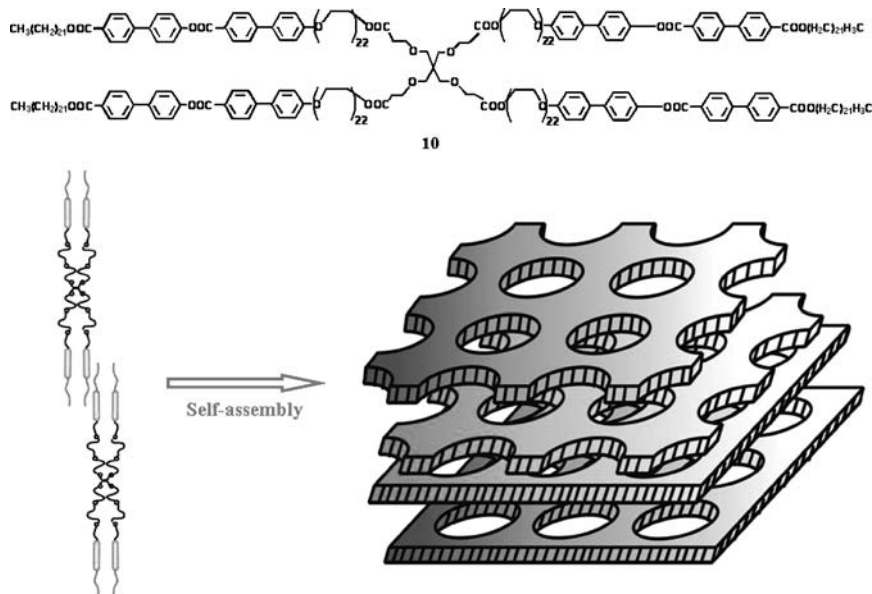


Fig. 9 Tetragonal perforated lamellar structure in an AB-BA sequence formed by tetra-branched triblock molecule

between the rod and PEO coil segments. The 3D lattice is built up of two interpenetrating centered 3D lattices. In comparison with the phase behavior of **9**, the remarkable feature of **10** is that attachment of coil-rod-coil molecules into a central point induces a perforated lamellar liquid crystalline phase with a 3D tetragonal symmetry that is thermodynamically stable. Upon melting of rod segments in **9**, there is adequate free volume for PEO to form a 2D hexagonal columnar mesophase. Attachment of four PEO chains to a central point, however, has the effect of reducing the freedom of movement for the flexible chains, which in turn suppresses the ability of the rod segments to form a columnar mesophase with a larger interfacial area. Consequently, certain supramolecular structures with reduced interfacial area, such as a perforated lamellar structures, are preferred over the columnar phase exhibited by the monomer.

Incorporation of a dendritic building block into the end of an incompatible linear chain gives rise to novel self-assembling systems because the molecule shares certain general characteristics of both block copolymers and small amphiphiles. Amphiphilic dendrimers containing an extended rigid rod block represent another class of self-assembling systems that are increasingly used for the construction of supramolecular architectures with well-defined shape. The introduction of a hydrophobic docosyl chain and hydrophilic dendrimer into each end of an extended rigid segment would give rise to a unique amphiphilic ABC triblock system consisting of a hydrophilic dendritic block,

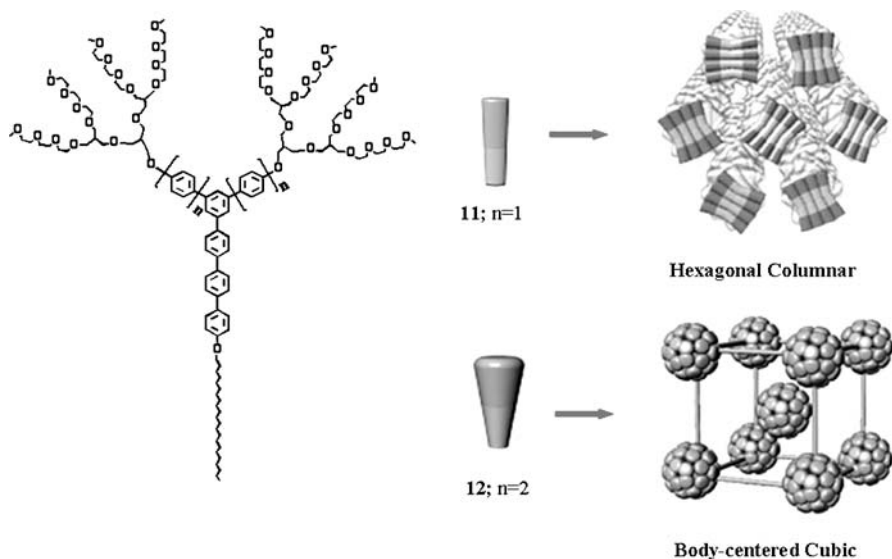


Fig. 10 Rod shape-dependent supramolecular structures

rigid aromatic, and hydrophobic docosyl chain [71]. The small-angle X-ray diffraction pattern of **11** displays sharp reflections that correspond to a 2D hexagonal columnar structure with a lattice constant of 8.1 nm. This dimension implies that the rod-like rigid segments arrange axially within a cross-sectional slice of the column, in which docosyl chains pack in an interdigitated fashion and distort conformationally (Fig. 10). In contrast, the small-angle X-ray diffraction patterns of **12** show a strong reflection together with a number of low intensity reflections at higher angles, indexed as a 3D body-centered cubic phase with a lattice parameter of 11.6 nm [72, 73]. Considering the space-filling requirement and cone-shaped building block, the radial arrangement of the rigid segments is expected to be the best way to close-pack the hydrophobic core, leading to a discrete nanostructure. Accordingly, **12** based on a more wedge-like aromatic segment can be described to self-organize into an optically isotropic cubic phase consisting of a 3D body-centered arrangement of discrete aggregates, as shown in Fig. 10.

Amphiphilic molecules consisting of oligo(phenylene vinylene) (OPV) asymmetrically end-substituted with a hydrophilic PEO segment and a hydrophobic alkyl chain induce self-assembly into both thermotropic and lyotropic lamellar liquid crystalline phases [74]. Depending on the length of PEO block, the mesostructures were controlled. When PEO chains are short, the amphiphilic molecule showed a mosaic birefringence texture from polarized optical microscopy, which is defined smectic B (S_B) mesophase. Increasing the length of PEO chain frustrates ordering of OPV aggregation and results

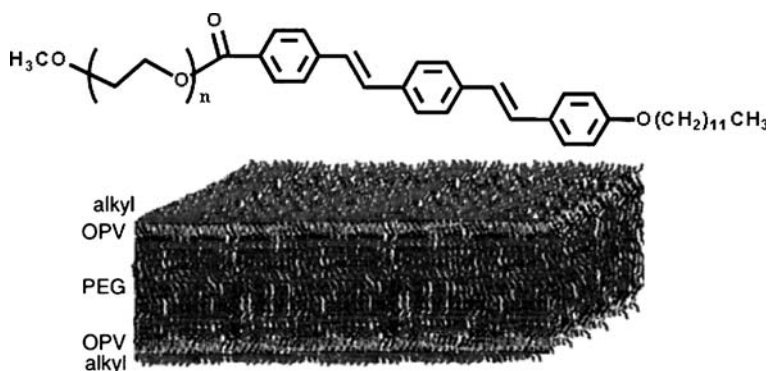


Fig. 11 Bilayer packing of amphiphilic OPV molecules. Reprinted with permission from [74]. © 2005 American Chemical Society

in smectic C (S_C) and smectic A (S_A) phases. The interlayer spacing is approximately equal to the fully extended lengths of the molecules, indicating significant interdigitation and/or tilt within a bilayer smectic structure. The X-ray data confirmed that OPV amphiphiles form an interdigitated bilayer smectic phase as shown in Fig. 11. Liquid crystallinity will be used to control OPV aggregation, influencing exciton mobility, fluorescence, and potentially leading to improved charge carrier mobility in heterojunction solar cells or enabling more efficient, polarized emission from organic light-emitting diodes.

Very recently, Lin et al. synthesized asymmetrical molecules consisting of a novel conjugated aromatic core containing fluorene, thiophene, and biphenyl groups and two kinds of PEO chains ($DP = 17$ and 44) on one side and alkoxy groups with different lengths ($-OC_8H_{17}$ and $-OC_{16}H_{33}$) on another side of the rigid core and their mesophases characterized [75]. Asymmetrical amphiphilic molecules based on short PEO chain ($DP = 17$) display the smectic phases. However, amphiphilic molecules based on longer PEO chain ($DP = 44$) show two kinds of columnar phases, hexagonal columnar and rectangular columnar. The immiscibility between the hydrophilic flexible chains and the hydrophobic rods leads to stronger lateral interaction of rigid rods and induces the smectic phases. By increasing the hydrophilic ethylene oxide units, the immiscibility increases and microphase separation is enhanced to form more order columnar phases.

3.2

ABA Coil-Rod-Coil Triblock Copolymers

In the case of symmetric coil-rod-coil molecule, the rod segment is connected with coil segments at both ends. This gives rise to the formation of the liquid crystalline structure with higher interfacial area in comparison with rod-coil diblock systems at similar coil volume fraction. For example, the

triblock molecule (13) with coil volume fraction, $f_{\text{coil}} = 0.47$ exhibits a bicontinuous cubic phase instead of smectic phase [76, 77]. Similarly to diblock rod-coil systems, increasing the volume fraction induces a hexagonal columnar mesophase as in the case of 14.

Remarkably, molecules with a longer length of coil (15) assemble into discrete supramolecular aggregates that spontaneously organize into a 3D tetragonal phase with a body-centered symmetry in the solid state and mesophase as determined by small-angle X-ray scattering. Based on X-ray data and density measurements, the inner core of the supramolecular aggregate is composed of the discrete rod bundle with a cylindrical shape of 5 nm in diameter and 3 nm in length. It is encapsulated with phase-separated PPO coils, which gives rise to the formation of non-spherical oblate aggregate (Fig. 12). The supramolecular rod bundles subsequently organize into a 3D body-centered tetragonal symmetry. The oblate shape of supramolecular aggregates is believed to be responsible for the formation of the unusual 3D tetragonal phase (M_{tet}). This unique phase behavior mostly originates from the anisotropic aggregation of rod segments with their long axes within microphase-separated aromatic domains. Consequently, rod bundles with puck-like cylindrical shape would give rise to oblate micelles, which can pack more densely into an optically anisotropic 3D tetragonal lattice, rather than an optically isotropic cubic lattice. These results demonstrate that the linear combination of flexible coils in both terminals of rod segment leads to discrete micellar aggregates that organize into a body-centered tetragonal liquid crystalline phase above a certain coil volume fraction.

Another possible way to manipulate the liquid crystalline structure could be provided by systematic variation of the rod length at constant rod-to-coil

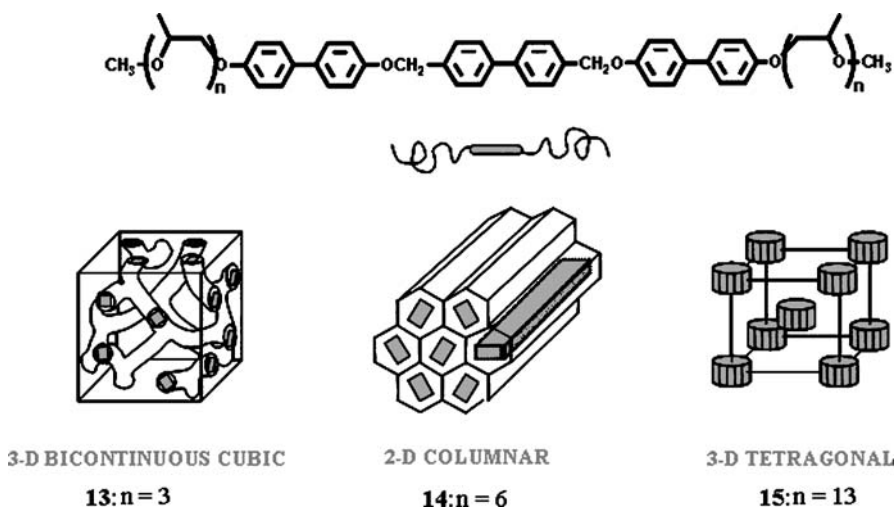
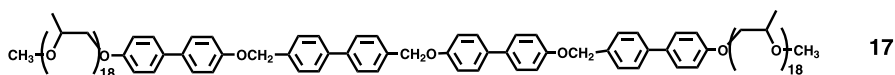
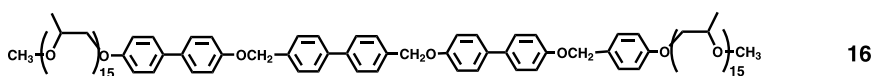


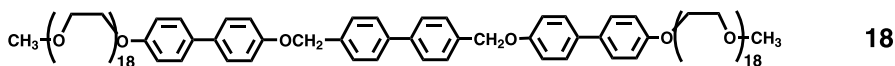
Fig. 12 Mesophase structures of the ABA coil-rod-coil triblock molecules

volume ratio. In particular, increasing the length of the rod segment should disturb the assembly of the rigid rod segments into discrete bundles due to larger rod-to-rod interactions. Rod-coil molecules **15**, **16**, and **17** have an identical rod-to-coil volume fraction ($f_{\text{rod}} = 0.22$). As mentioned above, the triblock molecule **15** based on three biphenyl units exhibits a tetragonal micellar liquid crystalline phase. In great contrast, the rod segment of **16** based on longer chain length self-assembles into a honeycomb-like layered liquid crystalline phase (HC) as a lower temperature mesophase in which hexagonally ordered perforations within a layer are filled by coil segments [78]. These layers, in turn, are stacked spontaneously in an ABAB fashion to generate a 3D hexagonal order. A DSC heating trace of **16** shows a crystalline melting transition at 136 °C, followed by a birefringent liquid crystalline phase that undergoes transformation into another liquid crystalline phase at 157 °C. On heating to 157 °C, the honeycomb-like mesophase transforms into a 3D tetragonal micellar liquid crystalline phase. On slow cooling from the isotropic liquid, the formation of fern-like domains growing in four directions with an angle of approximately 90°, which coalesce into a mosaic texture, could be easily observed using polarized optical microscopy, indicating the presence of a 3D tetragonal mesophase.



Further increasing the length of rod segment suppresses the formation of a 3D tetragonal mesophase, while inducing only a honeycomb-like liquid crystalline phase as in the case of the molecule **17**. These results indicate that the self-assembled 3D liquid crystalline phase changes significantly from organized rod bundles in a coil matrix (tetragonal structure) to organized coil perforations in rod layers (honeycomb structure) on increasing the rod length. This direct structural inversion is also accompanied by changing temperature. Therefore, changing temperature produces an effect similar to varying the molecular length. This example proves that the molecular length in rod-coil systems also has a large impact on the organized structure formed by self-assembly of rod-coil molecules.

The opposite way to modulate the supramolecular structure can be provided by variation in the coil structure while maintaining the rod segment constant. The influence of cross-sectional area of coil segment upon the self-assembly behavior were explored by ABA type coil-rod-coil molecules **15** and **18** that have identical coil volume fraction ($f_{\text{coil}} = 0.78$) relative to mesogenic rod segment, but different coil segments, i.e., PPO and PEO, re-



spectively [77]. As mentioned, **15** containing the PPO coils self-organizes into a 3D body-centered tetragonal lattice. In contrast, **18** shows significantly distinct self-assembly behavior. The optical microscopic observation of an arced pseudo-focal conic texture and the small-angle X-ray diffraction measurement both indicate that the supramolecular structures in mesophases are honeycomb-like lamellar structures where hexagonally perforated layers ($P6_3/mmc$ symmetry) are stacked in ABAB order.

The different self-assembly behavior of **15** and **18** with identical coil volume fraction points out the significance of coil cross-sectional area for the packing of rod segments. It can be rationalized by the consideration of coil density at the rod/coil interface as dependent upon coil cross-section. For a given space at the rod/coil junction, the coils with larger cross-sectional area cause more space crowding. The steric repulsion resulting from the space crowding leads to the stretched conformation of coils, leading to the coil stretching penalty [9c]. The morphological transition from continuous (the honeycomb-like lamellar structure of **18**) into discrete rod packing structures (the tetragonal structure of **15**) allows coils enough room to lower the coil conformational energy. Finally, self-assembly of rods can be fine-tuned in 3D nanospace since, in addition to coil volume fraction, coil cross-section is an independent parameter in building a variety of supramolecular structures.

A method for manipulating the size of the discrete nanostructures assembled from conjugated rod building blocks may be accessible by attaching chemically dissimilar, flexible dendritic wedges to their ends. Dumbbell-shaped molecules consisting of three biphenyls connected through vinyl linkages as a conjugated rod segment and aliphatic polyether dendritic wedges with different cross-sections (i.e., dibranched (**19**), tetrabranched (**20**) and hexabranched (**21**)) self-assemble into discrete bundles that organize into 3D superlattices [79]. Molecule **19**, based on a dibranched dendritic wedge, organizes into primitive monoclinic-crystalline and body-centered, tetragonal liquid crystalline structures, while molecules **20** and **21**, based on tetra- and hexabranched dendritic wedges, respectively, form only body-centered, tetragonal liquid crystalline structures (Fig. 13). X-ray diffraction experiments and density measurements showed that the rod-bundle cross-sectional area decreases with increasing cross-section of the dendritic wedges. The number of molecules per bundle decreases systematically with increasing cross-section of the dendritic wedge. Consequently, the size of the rod-bundle in cross-sectional area decreases in nanoscale dimension from 17.0 to 11.5 to 9.6 nm² for **19**, **20**, and **21**, respectively. The variation of rod bundle size in cross-section can be rationalized by considering both the steric repulsion between the bulky dendritic wedges and the nanophase separation between

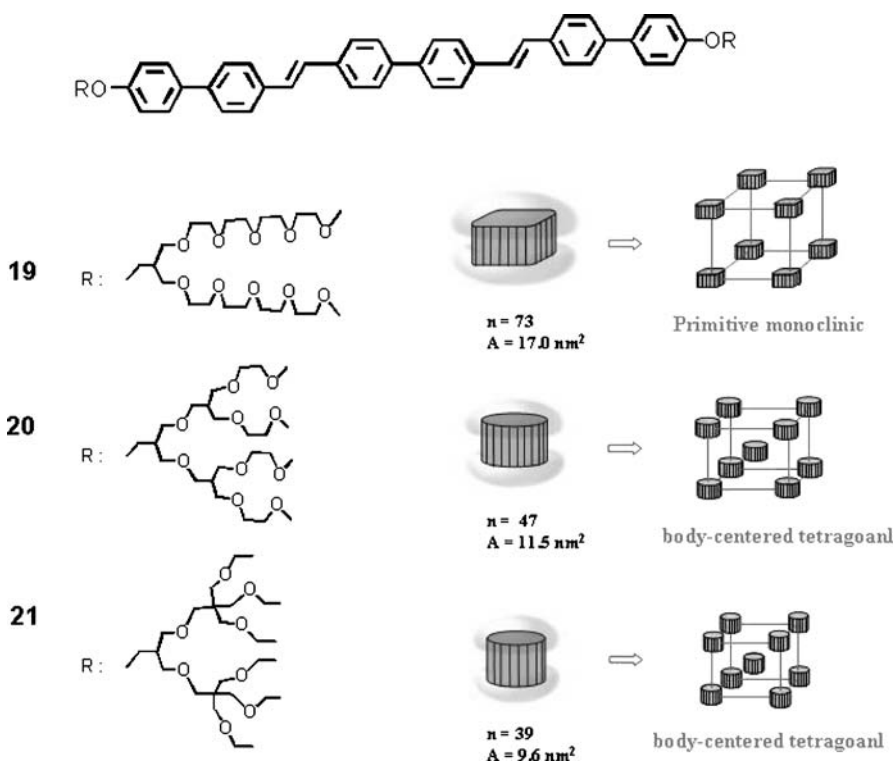


Fig. 13 Structural analysis of the supramolecular bundles assembled from molecular dumbbells 19–21

the dissimilar parts of the molecule [32, 33, 80, 81]. Anisotropic ordering of the rod building blocks in the molecule should exclude chemically dissimilar dendritic segments. Because dendritic wedges have a large cross-section, they will encounter strong repulsive forces when trying to accommodate the density of the ordered rod building blocks. These repulsive forces could balance the favorable aggregation of rod building blocks and generate the finite aggregation of dumbbell-shaped molecules. As the cross-sectional area of the dendritic wedges increases, so do the repulsive forces between them. Consequently, this increase in steric repulsion could give rise to smaller aggregates that allow more space for the dendritic building blocks to adopt a less strained conformation.

If supramolecular bundles are formed spontaneously in bulk films, by inclusion of appropriate reactive groups it should be possible to convert these into molecular objects by cross-linking, while maintaining the precise size and shape of the rod bundles. A coil-rod-coil triblock molecule **22** based on linear PPO ($f_{\text{coil}} = 0.73$) with a reactive rod block self-assembles into discrete rod bundles that are encapsulated by PPO coils and subsequently organize

into a 3D hexagonal close-packed structure ($P6_3/mmc$ space group symmetry) in the melt state, confirmed by optical polarized microscopy and X-ray diffraction measurements [82]. Cross-linking of **22** under UV irradiation of 254 nm in a liquid crystalline phase under nitrogen atmosphere for several hours resulted in the formation of a completely soluble macromolecule. GPC traces showed that the molecular weight appeared to be 270 kDa, with a narrow molecular weight distribution after polymerization. Small-angle X-ray scattering revealed several reflections corresponding to a 3D hexagonal lattice with essentially the same lattice constants as those of the coil-rod-coil molecule, indicative of the preservation of the ordered symmetry and the dimensions of the discrete objects after polymerization. On the basis of these lattice constants and measured density, the number of constituent units in each object was estimated to be approximately 112. The 3D hexagonal close-packed structure was observed to recover after isolation from the solutions and transform into an isotropic liquid in the bulk state in a reversible way, suggesting that the macromolecular objects are shape-persistent in solution as well as being an isotropic liquid phase of the bulk (Fig. 14).

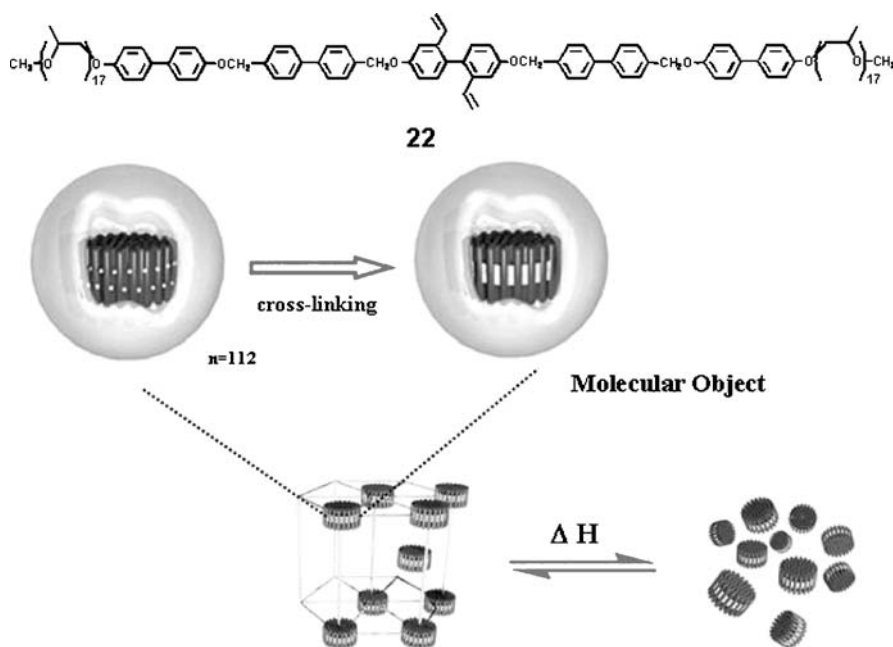
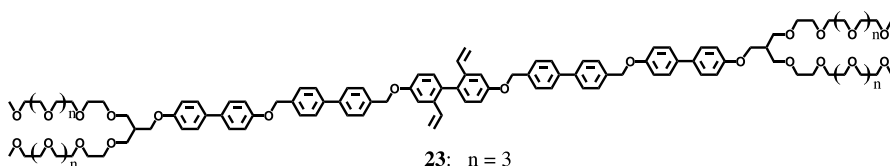


Fig. 14 Hexagonal close-packed liquid crystalline structure of the object and its transformation in to an isotropic liquid state

In contrast to linear coil, the triblock molecule **23**, consisting of bis(pentaethylene glycol) dendrons as coil segments at both ends of the rod with same rod building block, self-organizes into 2D columnar and 3D bicon-



tinuous cubic structures at the liquid crystalline state [83]. Photopolymerizations of **23** in liquid crystalline state proceed with preservation of the ordered supramolecular architectures and maintenance of the lattice dimensions. Photopolymerization of **23** in the bicontinuous cubic liquid crystalline state gives rise to a 3D ordered nanostructure, while in the hexagonal columnar liquid crystalline state it produces a 2D ordered nanostructure that in aqueous solution can be dispersed into individual nanofibers with a uniform diameter. The covalent stitching of reactive rod segments within the ordered state by photopolymerization offers a strategy to construct shape-persistent organic nanomaterials with well-defined size and shape, which potentially have applications in macromolecular electronics, nanoreactors, and hybrid nanomaterials.

A strategy to control the aggregation structure assembled from a rod building block may be accessible by incorporation of side groups into a rod block [84]. The side groups could lead to loose packing of the extended rod segments, which may modify the resulting supramolecular structure. A coil-rod-coil molecule (**24**) consisting of five biphenyl units connected through ether linkages as a rod block and PPO coils with the number of repeating units of 17, self-assembles into hexagonal perforated layers stacked in ABAB order in the melt. In contrast, a coil-rod-coil molecule (**25**) containing methyl

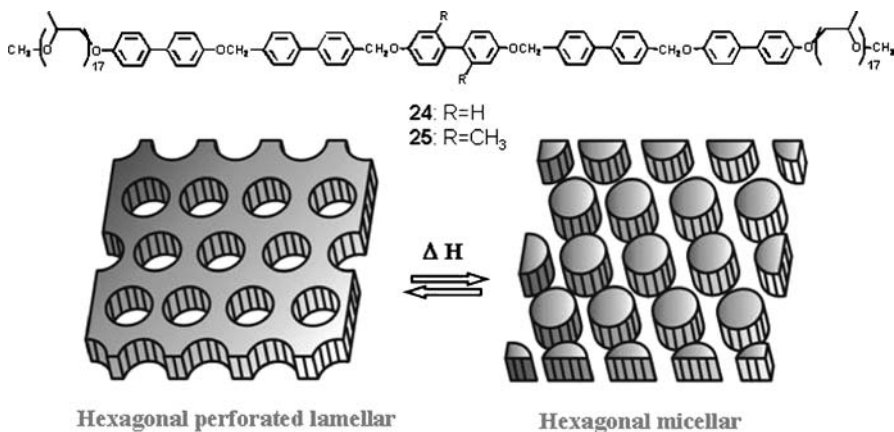


Fig. 15 Self-assembly of coil-rod-coil molecule **25** into the hexagonal perforated lamellar structure and subsequent conversion to hexagonal closed-packed bundles

side groups in its center shows an unusual supramolecular structural inversion, from perforated layers to discrete bundles, while maintaining a 3D hexagonal superlattice (Fig. 15). This phase transition on heating is most probably due to larger entropic contribution to the free energy associated with coil stretching [27, 85]. This indicates that the introduction of methyl side groups into a rod segment leads to the transformation of a 3D hexagonal perforated lamellar structure into a 3D hexagonally organized discrete bundles. This notable feature is that the incorporation of alkyl side groups into the center of a rod segment generates the structural inversion from organized coil perforations in rod layers to organized discrete rod-bundles in a coil matrix, while maintaining a 3D hexagonal superlattice. It is also remarkable that this structural inversion, retaining a 3D hexagonal superlattice, occurs directly without passing through any intermediate structures in a reversible way by changing the temperature. This abrupt structural change in rod-assembly may offer an attractive potential for use in supramolecular switch and thermal sensor.

3.3

BAB Rod–Coil–Rod Triblock Copolymers

Kato et al. reported on rod–coil–rod molecules consisting of rigid mesogenic cores and flexible PEO coils [86]. The small triblock molecule (**26**) was observed to exhibit smectic A liquid crystalline phase as determined by a combination of optical polarized microscopy and differential scanning calorimetry. The incorporation of LiCF_3SO_3 into the rod–coil–rod molecules shows significant mesophase stabilization. X-ray diffraction patterns revealed that complexation of **26** ($[\text{Li}^+]/[\text{EO}] = 0.05$) drastically reduces the layer spacing from 44 to 23 Å. This decrease is thought to be due to the interaction of the lithium salt with the ether oxygen, which results in a more coiled conformation of the PEO coil. Ion conductivities were also measured for complexes forming homeotropically aligned molecular orientation of the smectic phase. Interestingly, the highest conductivity was observed for the direction parallel to the layer (Fig. 16). However, the conductivities decrease in the polydomain sample, which disturbs the arrangement of ion paths. These results suggest that the self-organized rod–coil salt complexes can provide access to a novel strategy to construct ordered nanocomposite materials exhibiting low dimensional ionic conductivity.

Recently, rod–coil–rod triblock copolymers based on polydimethylsiloxane and polypeptide were reported by Rodriguez-Hernandez and coworkers [87]. In similar to rod–coil diblock copolymer with poly [poly(γ -benzyl-L-glutamate)], this triblock copolymer shows double hexagonal structure. The hexagonal array formed by α -helices remains stable at high temperatures. However, at a higher organization level the second hexagonal structure is lost at temperatures exceeding 160 °C. Moreover, this higher-level hexagonal

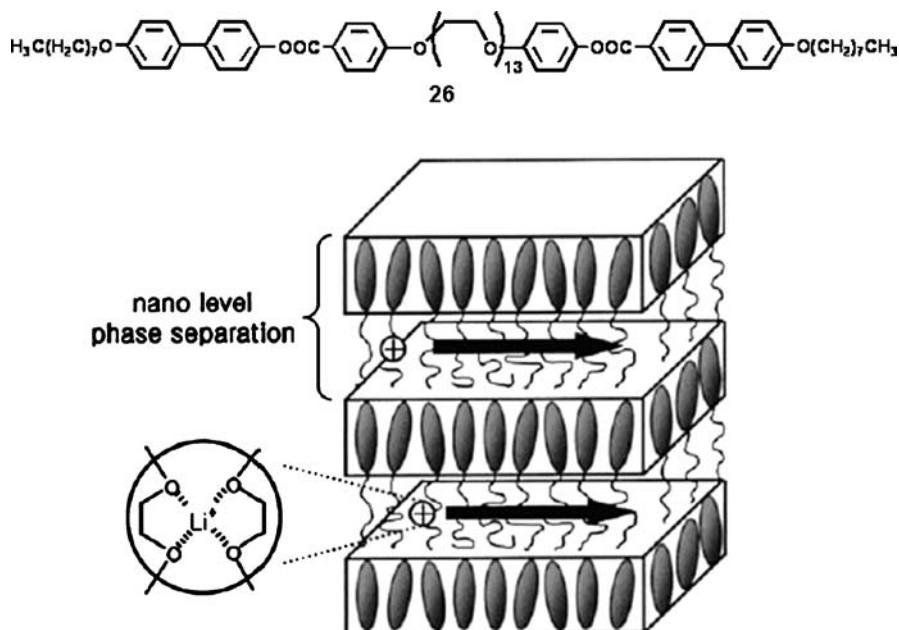


Fig. 16 Li^+ ion conduction for the complex of 26 in smectic A phase. Reprinted with permission from [86]. © 2000 American Chemical Society

structure can be reorganized on cooling indicating that this transition is reversible.

3.4

Novel Rod-Coil Triblock Copolymers

Precise control of supramolecular objects requires the rational design of molecular components, because the information determining their specific assembly should be encoded in their molecular architecture. Lee and coworkers reported on novel rod-coil molecules based on a hexa-*p*-phenylene rod and PEO chains that are fused together into a macrocyclic ring [88, 89]. The rod-coil macrocycle was observed to undergo double phase transitions in the crystalline state and to form ordered mesophases at higher temperature, as confirmed by differential scanning calorimetry. In the first crystalline state, 27 self-assembles into infinitely long ribbon-like 1D aggregates with uniform width and thickness. The cyclic geometry of the coil attached to one side of the rod would prohibit the 2D growth of a self-assembled structure. Instead, the aromatic rod segments should be strongly driven to aggregate in one dimension to produce a laterally stacked bilayer through microphase separation between the rod and coil segments, and π - π interactions. In the second crystalline state, the rod segments of 27 self-assemble into discrete ribbon-like

aggregates with a laterally stacked bilayer encapsulated by cyclic aliphatic chains in which the rod building blocks are arranged with their long axes parallel to each other. Subsequently, the ribbon nanostructures self-organize into a 3D body-centered orthorhombic superlattice (Fig. 17a). Both steric forces and crystallization of the rod segments are believed to play an important part in the formation of discrete ribbons [27]. The tendency of the rod building blocks to pack into a parallel arrangement accompanies a strong coil deformation on heating. To reduce the energetic penalty associated with coil deformation, while maintaining crystalline order of the rod segments, infinitely long ribbons would break up into discrete ribbons that allow coils to splay at the periphery of the supramolecular unit. In the birefringent mesophase of 27, small-angle X-ray scattering showed several reflections, corresponding to a 3D body-centered tetragonal superlattice with lattice parameters of 6.1 and 5.9 nm. Wide-angle scattering showed only a broad halo, indicative of liquid crystalline order of the rod segments within domains. On cooling from the optically isotropic mesophase, straight lines growing in four directions with an angle of 90° could be observed in the polarized optical microscope with a final development of mosaic texture, indicative of the presence of a 3D non-cubic lattice [76]. On further heating to the optically isotropic mesophase, the small-angle X-ray scattering pattern showed three sharp peaks that could be indexed as a 3D body-centered cubic phase with a lattice parameter of 5.7 nm. According to the number of molecules per aggregate, by using the lattice constants and densities, aggregates of 27 were estimated to contain about 40 molecules each. Considering microphase separation between the rod and coil segments, the aggregation of 40 rod-coil macrocyclic molecules in an ag-

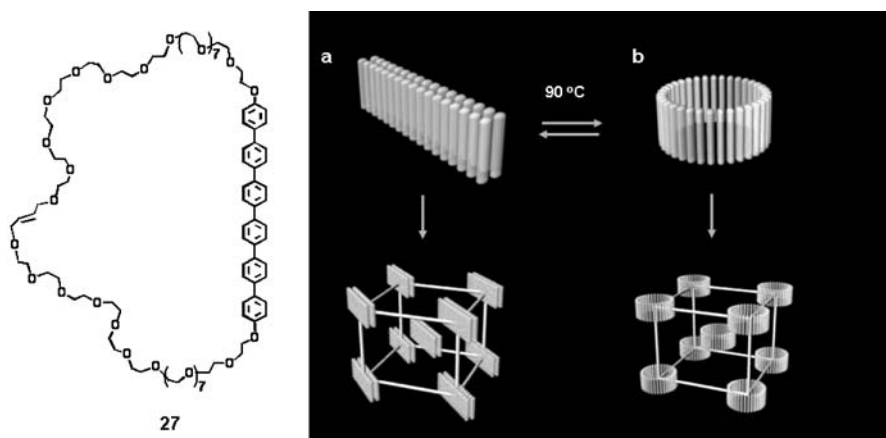


Fig. 17 Supramolecular architectures from self-assembly of rod-coil macrocycles. **a** Body-centered orthorhombic structures from ribbon-like aggregates; **b** body-centered tetragonal structures from barrel-like aggregates

gregate can be viewed as generating a barrel-like supramolecular structure in which the rods are aligned axially with their preferred direction, and both the interior and exterior of the barrel are filled by the coil segments (Fig. 17b). These results indicate that a flat discrete ribbon-like aggregate transforms into a curved barrel-like structure on crystal melting of the rod segments. This transformation may be rationalized by considering end-to-end connection by rolling of the discrete ribbon [90]. With increasing temperature, space crowding of coil segments would be larger because of greater thermal motion of the flexible chains. A ribbon-like ordering of the rod segments would confine flexible coil segments to a flat interface, forcing a strong deformation of the flexible coils and making the system energetically unfavorable. To release this deformation without sacrificing anisotropic order of the rod segments, the flat ribbons would roll to form curved barrels.

Tschierske and coworkers reported on new complex liquid crystalline phases of polyphilic block molecules or their metal complex [91–93]. These triblock rod-coil molecules consist of a rod-like *p*-terphenylene unit, and two hydrophobic alkyl chains at both ends of the rod, and oligo(ethylene glycol) with a terminal carbohydrate unit at a lateral position of the rod [94]. Depending on the size of the hydrophilic and hydrophobic segments, a series of unusual liquid crystalline phases were detected (Fig. 18). When the carbohydrate unit is directly conjugated to the rod building block, a simple smectic (S_A) phase was observed. In this liquid crystalline phase, the molecules are

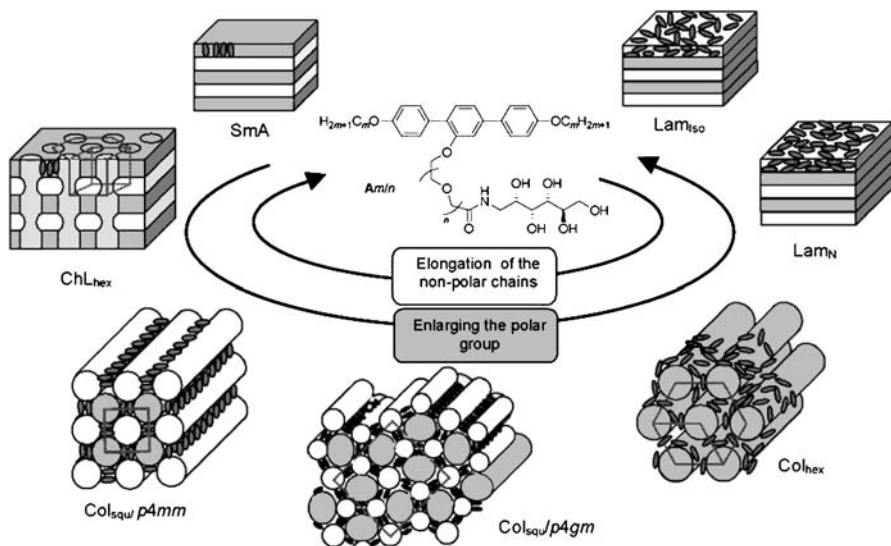


Fig. 18 Supramolecular architectures from self-assembly of facial rod-coil molecules with lateral hydrophilic groups as a function of the size of polar lateral and hydrophobic terminal groups. Reprinted with permission from [94]. © 2005 American Chemical Society

organized in layers, where the terphenyl units and the lateral carbohydrate units are incorporated in the layer and these sublayers are separated by layers of alkyl chains. Increasing the space unit (oligo(ethylene glycol)) transformed smectic mesophase into a hexagonal channeled layer phase (ChL_{hex}). This mesophase appears almost completely black between crossed polarizers and shows a very high viscosity, indicating an optically uniaxial mesophase with a 3D lattice. Small-angle X-ray diffraction pattern shows five spots that could be indexed as a 3D hexagonal lattice ($P6/mmm$). This mesophase consists of alternating layers of aromatic units and aliphatic chains, penetrated at right angles by columns with undulating profiles containing the polar lateral groups. Accordingly, the structure consists of layers perforated by an array of polar channels, which are arranged on a 2D hexagonal lattice.

When the space units were increased further, rod-coil molecules form square columnar mesophases confirmed by optical polarized microscopy and X-ray diffraction pattern. The polar column is located inside the square, providing strong attractive intermolecular interactions via hydrogen bonding and the hydrophobic columns containing alkyl chains are at the corners interconnecting the aromatic rods end-to-end. For the columnar mesophases, the rigid-rod segments tend to restrict the side length of the polygons within relatively narrow limits, giving rise to columns with a well-defined polygonal shape. The lateral chains fill the interior of the polygons; the terminal chains form the corners of these polygons and connect the rigid rods. Thus, the number of sides of the polygons critically depends on the volume of the lateral chain and the length of the molecule. Extending the hydrophilic chain, raising the temperature, or reducing the alkyl chain length leads to a transition from square to hexagonal columnar phases. Due to amphotropic characteristics of rod-coil molecules, new types of laminated mesophases also were induced by solvent (Fig. 18).

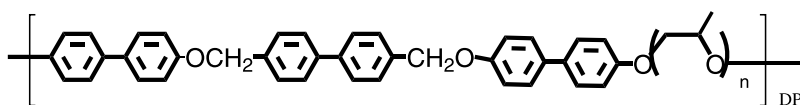
4

Multiblock Rod-Coil System

4.1

Main-Chain Rod-Coil Copolymers

The rod-coil approach as a means to manipulate supramolecular structure as a function of rod volume fraction was reported to be extended to main chain multiblock copolymer systems, which generate bicontinuous cubic and hexagonal columnar mesophases depending on the rod-to-coil volume fraction [95, 96]. For example, rod-coil multiblock copolymer (**28**) based on short length of coil (rod volume fraction, $f_{\text{rod}} = 0.38$) exhibits a bicontinuous cubic mesophase, while copolymer (**29**) based on higher coil volume fraction ($f_{\text{rod}} = 0.29$) shows a hexagonal columnar mesophase. A notable feature



$$28 \quad n = 12$$

$$29 \quad n = 18$$

of this system is the ability of the main-chain liquid crystalline polymers based on a rod building block to self-assemble into ordered structures with curved interfaces. Formation of supramolecular columnar and bicontinuous cubic assemblies in the rod-coil copolymers is in marked contrast to the general behavior of conventional liquid crystalline polymers based on rod-like mesogens and segmented copolymers based on alternating rigid and flexible segments [97, 98]. Formation of the ordered structures with interfacial curvature from the main-chain rod-coil copolymers can be rationalized by considering entropic penalties associated with coil stretching and anisotropic arrangement of rod segments. Bulky PPO coils induce curvature at the rod/coil interface (arising from the connectivity of the rod and coils), constraint of constant density, and minimization of coil stretching. At the interface separating the rod and coil domains in the layered smectic structure, the relatively smaller area per junction favored by rod block results in chain stretching of the coil block, which is energetically unfavorable. Therefore, the rod-coil copolymers self-assemble into bicontinuous cubic or hexagonal columnar structures with larger interfacial area, instead of a layered smectic structure.

In contrast to this, another strategy for manipulating the supramolecular structure at constant rod-to-coil volume ratio can also be accessible by varying the number of grafting sites per rod, which might be closely related to the grafting density at the interface separating rod and coil segments. For this reason, **30**, **31** and **32**, with rod-coil repeating units consisting of three biphenyl units connected by methylene ether linkages as the rod block and PPO with 13 PO repeating units as the coil block, were prepared [99]. All of the oligomers are self-organized into ordered supramolecular structures that differ significantly on variation of the number of repeating units, as confirmed by X-ray scattering. The molecule **30** shows a bicontinuous cubic liquid crystalline structure. In contrast, the molecule **31** shows a 2D rectangular crystalline and a tetragonal columnar (col_t) liquid crystalline structures, while the molecule **32** displays a hexagonal columnar structure in both their solid state and mesophase (Fig. 19). These results show that self-assembled liquid crystalline structures, from 3D bicontinuous cubic, 2D tetragonal, to 2D hexagonal lattices are formed by rod-coil structures that differ only in the number of repeating units.

This interesting variation of self-assembled structures, at an identical rod-to-coil volume ratio, can be explained by considering the density of grafting sites at the interface separated by rod and coil. On increasing the number

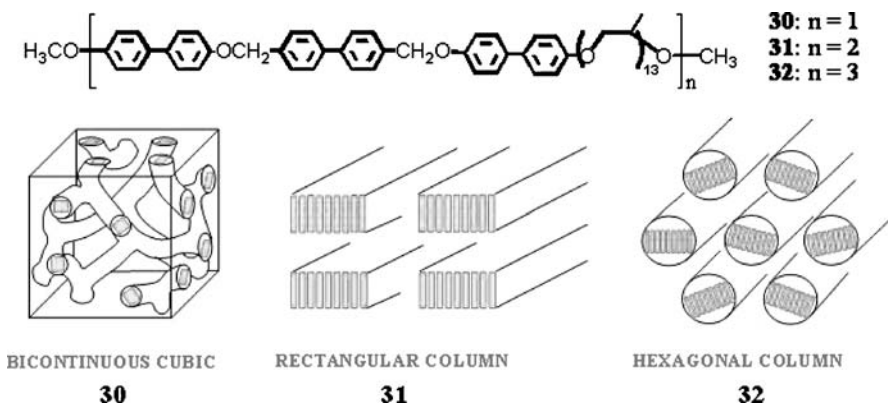


Fig. 19 Mesophase of the rod-coil multiblock molecules depending on rod-coil repeating units

of rod-coil repeating units, the density of grafting sites at the interface will be increased due to an increase in the average number of coils grafted to a rod, which results in strong entropic penalty associated with coil stretching at the rod-coil interface. To reduce this coil stretching, a bicontinuous cubic structure of the monomer would break up into 2D cylindrical domains in which less confinement and deformation of coil segments occur. These results demonstrate that systematic variation of the number of repeating units in the rod-coil multiblock oligomers can provide a strategy to regulate the liquid crystalline phase, from bicontinuous cubic, 2D tetragonal columnar, to 2D hexagonal columnar structures.

Picken et al. recently reported on the phase behavior of a series of rod-coil multiblock copolymers comprised of alternating poly(*p*-phenylene terephthalamide) as a rod building block and polyamide blocks as a coil part [100]. When the mole fraction of rod parts exceeds 0.5 these polymers show lyotropic liquid crystalline structure in concentrated sulfuric acid solution. The critical concentration for the formation of a nematic phase increases with increasing fraction of the flexible fragments in the block copolymer, and coupling of flexible chains to rod-like oligomers increases the stability of the liquid crystalline phase. This means that the liquid crystallinity involves induced orientation of the flexible polyamide coils. The incorporation of aramid blocks in the copolymer induces stretching of the flexible coils, and this stretching will make the copolymer stiffer.

4.2

Side-Chain Rod-Coil Copolymers

A novel strategy for manipulating the supramolecular structure can also be accessed by converting the rod-coil monomer into a side chain polymer. Lee

et al. reported on the supramolecular behavior of the liquid crystalline state of rod-coil monomers and their corresponding polymer, consisting of a rigid rod made up of two biphenyls connected through ester linkages and flexible PPO coils (Fig. 20) [101]. Polymerization of the rod-coil monomer into a side chain polymer gives rise to a large structural transformation from 2D hexagonal to 3D cubic structures. Polymerization of the acryl group stitches coil segments into a polymer backbone and produces selective shrinkage of coil domains in the microphase-separated supramolecular structure. This is responsible for the transformation of the hexagonal columnar structure exhibited by the monomer into a bicontinuous cubic structure that allows less volume for the coil upon polymerization.

Incorporation of aromatic rigid-rod segments in the side chain of block copolymer can play a role in forming well-ordered nanostructures. Finkelmann et al. reported that block copolymer consisting of poly(hexyl methacrylate) as a coil and an azobenzene moiety as a rod showed liquid crystalline mesophases including smectic A and bicontinuous cubic phase [102]. Based on TEM experiments, the smectic layers of rod units are oriented either parallel or perpendicular to the lamellar morphology. The deformation of the anisotropic phase structure leads to the formation of a gyroid morphology. Hayakawa et al. also reported on side-chain rod-coil block copolymer composed of a poly(styrene-*b*-substituted isoprene) with an oligothiophene derivatives [103]. DSC and X-ray data showed characteristics of a liquid-crystalline smectic mesophase of the π -stacked oligothiophene blocks. TEM images indicated that the phase-separated polystyrene and polyisoprene with oligothiophene-modified side chain were aligned layer by layer due to the self-assembly characteristic of the diblock copolymer. The combination of a liquid-crystal phase and phase-separated nanodomain structures formed extremely regular hierarchical structures.

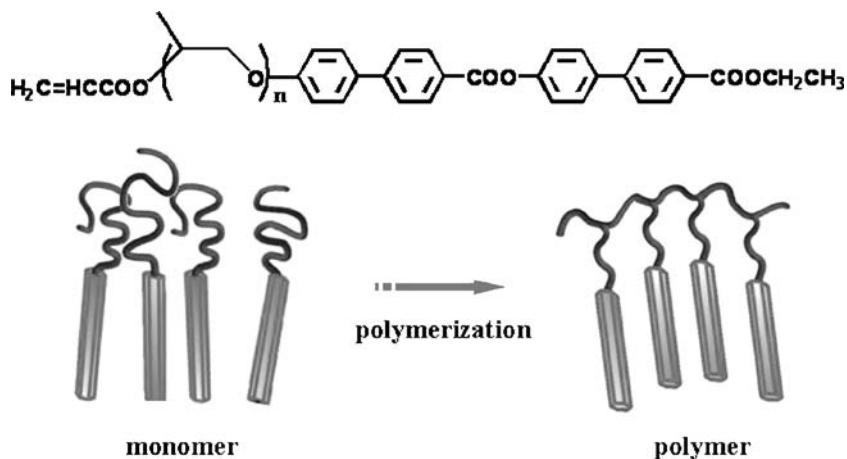


Fig. 20 Side-chain rod-coil polymer from polymerization

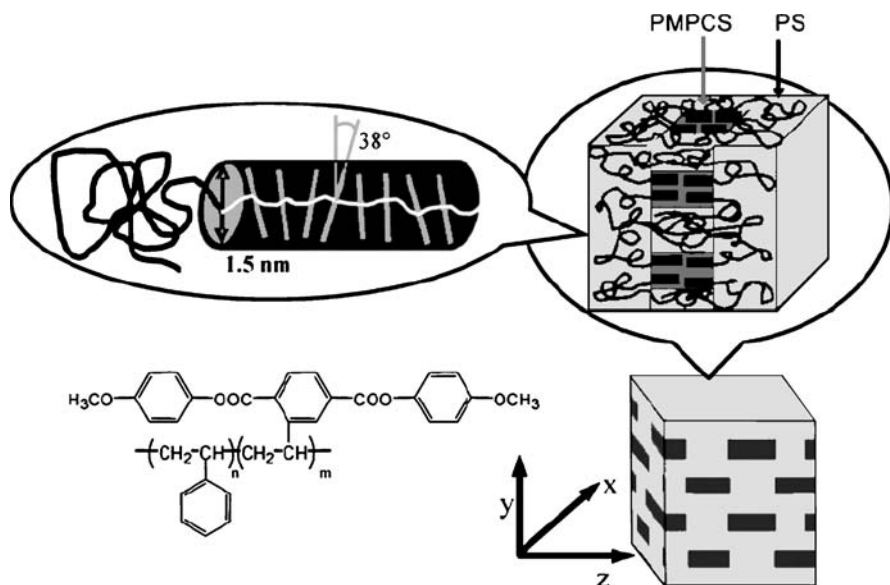


Fig. 21 Perforated lamellar structure hierarchically formed by poly(styrene-*b*-(2,5-bis[4-methoxyphenyl] oxycarbonyl)styrene) structure. Reprinted with permission from [107]. © 2005 American Chemical Society

By laterally linking aromatic mesogens directly to polymer backbones, mesogen-jacketed liquid crystalline polymers as a rod-coil copolymer can be achieved [104–106]. Zhou and coworkers reported on the supramolecular structures of these type of rod-coil copolymers composed of poly(styrene-*b*-(2,5-bis[4-methoxyphenyl] oxycarbonyl)styrene) [107]. The strong interaction between the side-chain mesogens and polymer backbone induces formation of rigid columns of mesogens. The macromolecular columns possess orientational order and then these rigid columns self-assemble into a columnar nematic of hexagonal mesophase. On increasing the volume fraction of polystyrene blocks, the mesophases change from lamellar to perforated lamellar structures, where the polystyrene perforates the macromolecular rigid column layer of poly(2,5-bis[4-methoxyphenyl]oxycarbonyl)styrene (Fig. 21).

5 Conclusions

A variety of different supramolecular structures can be formed by self-assembly of mesogenic rod building blocks with terminally attached polyether coils. This unique phase behavior seems to originate from a combination of organizing forces. These include the mutual repulsion of the dissimilar blocks and packing constraints imposed by the connecting of each block, and the

tendency of the rod block to form orientational order. The incorporation of different rod-like segments such as helical rods, low molar mass mesogenic rods, and conjugated rods as a part of the main chain in rod-coil molecular architecture has already proven to be an effective way to manipulate supramolecular structures in nanoscale dimensions. Depending on the relative volume fraction of rigid and flexible segments, and the chemical structure of these segments, rod-coil copolymers and their low molar mass homologs self-assemble into a variety of supramolecular structures through the combination of shape complementarity and microphase separation of rod and coil segments as an organizing force. The supramolecular structures assembled by rod segments in rod-coil systems include sheets, cylinders, finite nanostructures, and even perforated sheets that organize into 1D, 2D, and 3D superlattices, respectively. It should be noted that self-assembly can be used to prepare well-defined macromolecular nanoobjects that are not possible to prepare by conventional synthetic methodologies, when the rod-coil copolymers self-assemble into discrete supramolecular structures. In this respect, many synthetic strategies have been developed that allow the incorporation of functional rod segments into well-defined rod-coil architectures for specific properties. Electron transfer, second harmonic generation, and piezoelectricity have been reported for supramolecular structures of rod-coil copolymers containing conjugated rods or highly polar end groups [108–110]. Many more rod-coil systems are expected to be developed soon for possible applications as diverse as molecular materials for nanotechnology, supramolecular reactors, periodic porous materials, transport membranes, and biomimic materials.

References

1. Lehn JM (1995) *Supramolecular chemistry, concepts and perspective*. VCH, Weinheim
2. Lee M, Cho BK, Zin WC (2001) *Chem Rev* 101:3869
3. Klok HA, Lecommandoux S (2001) *Adv Mater* 13:1217
4. Stupp SI, Pralle MU, Tew GN, Li L, Sayar M, Zubarev ER (2000) *MRS Bull* 42
5. Loos K, Munoz-Guerra S (2000) *Microstructure and crystallization of rigid-coil comblike polymers and block copolymers*. In: Ciferri A (ed) *Supramolecular polymers*, Chap 7. Dekker, New York
6. Ryu JH, Cho BK, Lee M (2006) *Bull Korean Chem Soc* 27:1270
7. Collings PJ, Hird M (1997) *Introduction to liquid crystals: chemistry and physics*. Taylor and Francis, London
8. Tschierske C (2001) *J Mater Chem* 11:2647
9. Kato T, Mizoshita N, Kishimoto K (2006) *Angew Chem Int Ed* 45:38
10. Mingos DMP (1999) *Liquid crystal II*. Springer, Berlin Heidelberg New York
11. Föster S, Plantenberg T (2002) *Angew Chem Int Ed* 41:688
12. Föster S, Antonietti M (1998) *Adv Mater* 10:195
13. Khandpur AK, Föster S, Bates FS, Hamley IW, Ryan AJ, Bras W, Almdal K, Mortensen K (1995) *Macromolecules* 28:8796

14. Zeng F, Zimmerman SC (1997) *Chem Rev* 97:1681
15. Brunsveld L, Folmer BJB, Meijer EW, Sijbesma RP (2001) *Chem Rev* 101:4071
16. Hennigar TL, MacQuarrie DC, Losier P, Rogers RD, Zaworotko MJ (1997) *Angew Chem Int Ed* 36:972
17. Kaes C, Hosseini MW, Rickard CEF, Skelton BW, White AH (1998) *Angew Chem Int Ed* 37:920
18. Cui Y, Lee SJ, Lin W (2003) *J Am Chem Soc* 125:6014
19. Tschierske C (1998) *J Mater Chem* 8:1485
20. Berresheim AJ, Müller B, Müllen K (1999) *Chem Rev* 99:1747
21. Steffen W, Köhler B, Altmann M, Scherf U, Stitzer K, Loye HC, Bunz UHF (2001) *Chem Eur J* 7:117
22. Jeneckhe SA, Chen XL (1999) *Science* 283:372
23. Lee M, Yoo YS (2002) *J Mater Chem* 12:2161
24. Stupp SI (1998) *Curr Opin Colloid Interface Sci* 3:20
25. Semenov AN, Vasilenko SV (1986) *Sov Phys JETP* 63:70
26. Semenov AN (1991) *Mol Cryst Liq Cryst* 209:191
27. Williams DRM, Fredrickson GH (1992) *Macromolecules* 25:3561
28. Halperin A (1990) *Macromolecules* 23:2724
29. Lee M, Oh NK (1996) *J Mater Chem* 6:1079
30. Lee M, Oh NK, Choi MG (1996) *Polym Bull* 37:511
31. Lee M, Oh NK, Zin WC (1996) *Chem Commun*, p 1787
32. Lee M, Cho BK, Kim H, Zin WC (1998) *Angew Chem Int Ed* 37:638
33. Lee M, Cho BK, Kim H, Yoon JY, Zin WC (1998) *J Am Chem Soc* 120:9168
34. Hamley IW, Ropp KA, Rosedale JH, Bates FS, Almdal K, Mortensen K (1993) *Macromolecules* 26:5959
35. Bates FS, Schulz MF, Khandpur AK, Foster S, Rosedale JH, Almdal K, Mortensen K (1994) *Faraday Discuss Chem Soc* 98:7
36. Park MH, Ryu JH, Lee E, Han KH, Chung YW, Cho BK, Lee M (2006) *Macromol Rapid Commun* 27:1684
37. Radzilowsk JL, Wu JL, Stupp SI (1993) *Macromolecules* 26:879
38. Radzilowsk JL, Stupp SI (1994) *Macromolecules* 27:7747
39. Radzilowsk JL, Carragher BO, Stupp SI (1997) *Macromolecules* 30:2110
40. Stupp SI, Lebonheur V, Walker K, Li LS, Huggins KE, Keser M, Amstutz A (1997) *Science* 276:384
41. Zubarev ER, Pralle MU, Li L, Stupp SI (1999) *Science* 283:523
42. Zubarev ER, Pralle MU, Sone ED, Stupp SI (2001) *J Am Chem Soc* 123:4105
43. Li W, Wang H, Yu L, Morkved TL, Jaeger HM (1999) *Macromolecules* 32:3034
44. Wang H, Wang HH, Urban VS, Littrell KC, Thiyagarajan P, Yu L (2000) *J Am Chem Soc* 122:6855
45. Kim JK, Hong MK, Ahn JH, Lee M (2005) *Angew Chem Int Ed* 44:328
46. Ungar G, Liu Y, Zeng X, Percec V, Cho WD (2003) *Science* 299:1208
47. Kato T, Matsuoka T, Nishii M, Kamikawa Y, Kanie K, Nishimura T, Yashima E, Ujiie S (2004) *Angew Chem Int Ed* 43:1969
48. Fréchet JMJ (2002) *Proc Natl Acad Sci USA* 99:4782
49. Bur AJ, Fetters LJ (1976) *Chem Rev* 76:727
50. Fetters LJ, Yu H (1971) *Macromolecules* 4:385
51. Aharoni SM (1979) *Macromolecules* 12:94
52. Aharoni SM, Walsh EK (1979) *Macromolecules* 12:271
53. Aharoni SM (1980) *J Polym Sci Polym Phys Ed* 18:1439
54. Chen JT, Thomas EL, Ober CK, Hwang SS (1995) *Macromolecules* 28:1688

55. Chen JT, Thomas EL, Ober CK, Mao G (1996) *Science* 273:343
56. Park JW, Thomas EL (2003) *Adv Mater* 15:585
57. Park JW, Thomas EL (2004) *Macromolecules* 37:3532
58. van der Veen MH, de Boer B, Stalmach U, van de Wetering KI, Hadziioannou G (2004) *Macromolecules* 37:3673
59. Gallot B (1996) *Prog Polym Sci* 21:1035
60. Zhang G, Fournier MJ, Mason TL, Tirrell DA (1992) *Macromolecules* 25:3601
61. Yu SM, Conticello VP, Zhang G, Kayser C, Fournier MJ, Mason TL, Tirrell DA (1997) *Nature* 389:167
62. Klok HA, Langenwalter JF, Lecommandoux S (2000) *Macromolecules* 33:7819
63. Lecommandoux S, Achard MF, Langenwalter JF, Klok HA (2001) *Macromolecules* 34:9100
64. Minich EA, Nowak AP, Deming TJ, Pochan DJ (2004) *Polymer* 45:1951
65. Hanski S, Houbenov N, Ruokolainen J, Chondronicola D, Iatrou H, Hadjichristidis N, Ikkala O (2006) *Biomacromolecules* 7:3379
66. Stadler R, Auschra C, Beckmann J, Krappe U, Voigt-Martin I, Leibler L (1995) *Macromolecules* 28:3080
67. Lee M, Lee DW, Cho BK, Yoon JY, Zin WC (1998) *J Am Chem Soc* 120:13258
68. Schwab M, Stuehn B (1996) *Phys Rev Lett* 76:924
69. Sakamoto N, Hashimoto T, Han CD, Vaidya N (1997) *Macromolecules* 30:1621
70. Oh NK, Zin WC, Im JH, Ryu JH, Lee M (2004) *Chem Commun*, p 1092
71. Jang CJ, Ryu JH, Lee JD, Sohn D, Lee M (2004) *Chem Mater* 16:4226
72. Percec V, Cho WD, Ungar G, Yearley DJP (2001) *J Am Chem Soc* 123:1302
73. Yearley DJP, Ungar G, Percec V, Holerca MN, Johansson G (2000) *J Am Chem Soc* 122:1684
74. Hulvat JF, Sofos M, Tajima K, Stupp SI (2005) *J Am Chem Soc* 127:366
75. Lin HC, Lee KW, Tsai CM, Wei KH (2006) *Macromolecules* 39:3808
76. Lee M, Cho BK, Jang YG, Zin WC (2000) *J Am Chem Soc* 122:7449
77. Cho BK, Chung YW, Lee M (2005) *Macromolecules* 38:10261
78. Cho BK, Lee M, Oh NK, Zin WC (2001) *J Am Chem Soc* 123:9677
79. Lee M, Jeong YS, Cho BK, Oh NK, Zin WC (2002) *Chem Eur J* 8:876
80. Henglein A (1989) *Chem Rev* 89:1861
81. Murray BC, Norris DJ, Bawendi MG (1993) *J Am Chem Soc* 115:8706
82. Jin LY, Ahn JH, Lee M (2004) *J Am Chem Soc* 126:12208
83. Jin LY, Bae J, Ryu JH, Lee M (2006) *Angew Chem Int Ed* 45:650
84. Jin LY, Bae J, Ahn JH, Lee M (2005) *Chem Commun*, p 1197
85. Müller M, Schich M (1996) *Macromolecules* 29:8900
86. Ohtake T, Ogasawara M, Ito-Akita K, Nishina N, Ujie S, Ohno H, Kato T (2000) *Chem Mater* 12:782
87. Ibarboure E, Rodríguez-hernández J, Papon E (2006) *J Polym Sci Part A Polym Chem* 44:4668
88. Yang WY, Ahn JH, Yoo YS, Oh NK, Lee M (2005) *Nat Mater* 4:399
89. Yang WY, Lee E, Lee M (2006) *J Am Chem Soc* 128:3484
90. In M, Aguerre-Chariol O, Zana R (1999) *J Phys Chem B* 103:7747
91. Chen B, Baumeister U, Diele S, Das MK, Zeng XB, Ungar G, Tschierske C (2004) *J Am Chem Soc* 126:8608
92. Chen B, Zeng XB, Baumeister U, Diele S, Ungar G, Tschierske C (2004) *Angew Chem Int Ed* 43:4621
93. Chen B, Zeng XB, Baumeister U, Ungar G, Tschierske C (2005) *Science* 307:96

94. Chen B, Baumeister U, Pelzl G, Das MK, Zeng XB, Ungar G, Tschierske C (2005) *J Am Chem Soc* 127:16578
95. Lee M, Cho BK, Kang YS, Zin WC (1999) *Macromolecules* 32:7688
96. Lee M, Cho BK, Kang YS, Zin WC (1999) *Macromolecules* 32:8531
97. Eisenbach CD, Heinemann T, Ribbe A, Stadler E (1994) *Macromol Symp* 77:125
98. Osaheni JA, Jenekhe SA (1995) *J Am Chem Soc* 117:7389
99. Lee M, Cho BK, Oh NK, Zin WC (2001) *Macromolecules* 34:1987
100. de Ruijter C, Jager WF, Li L, Picken SJ (2006) *Macromolecules* 39:4411
101. Cho BK, Choi MG, Zin WC, Lee M (2002) *Macromolecules* 35:4845
102. Schneider A, Zanna JJ, Yamada M, Finkelmann H, Thomann R (2000) *Macromolecules* 33:649
103. Hayakawa T, Horiuchi S (2003) *Angew Chem Int Ed* 42:2285
104. Zhou QF, Zhu XL, Wen ZQ (1989) *Macromolecules* 22:491
105. Zhang D, Liu YX, Wan XH, Zhou QF (1999) *Macromolecules* 32:5183
106. Gopalan P, Ober CK (2001) *Macromolecules* 34:5120
107. Tenneti KK, Chen X, Li CY, Tu Y, Wan X, Zhou QF, Sics I, Hsiao BS (2005) *J Am Chem Soc* 127:15481
108. Pralle MU, Whitaker CM, Braun PV, Stupp SI (2000) *Macromolecules* 33:3550
109. Tew GN, Pralle MU, Stupp SI (2000) *Angew Chem Int Ed* 39:517
110. Stalmach U, de Boer B, Vidélot C, van Hutten PF, Hadziioannou G (2000) *J Am Chem Soc* 122:5464